HHS Public Access

Author manuscript

Arthritis Rheum. Author manuscript; available in PMC 2015 May 19.

Published in final edited form as:

Arthritis Rheum. 2013 May ; 65(5): 1335–1346. doi:10.1002/art.37859.

Thymic Stromal Lymphopoietin Is Up-Regulated in the Skin of Patients With Systemic Sclerosis and Induces Profibrotic Genes and Intracellular Signaling That Overlap With Those Induced by Interleukin-13 and Transforming Growth Factor β

Romy B. Christmann, MD, PhD[1], **Allison Mathes, BS**[1], **Alsya J. Affandi, MSc**[2], **Cristina Padilla, MS**[1], **Banafsheh Nazari, MSc**[1], **Andreea M. Bujor, MD**[1], **Giuseppina Stifano, MD**[1], and **Robert Lafyatis, MD**[1]

[1]Boston University School of Medicine, Boston, Massachusetts [2]Boston University School of Medicine, Boston, Massachusetts, and University Medical Center Utrecht, Utrecht, The Netherlands

Abstract

Objective—To explore the expression of thymic stromal lymphopoietin (TSLP) in patients with diffuse cutaneous systemic sclerosis (dcSSc) and compare its effects in vivo and in vitro with those of interleukin-13 (IL-13) and transforming growth factor β (TGFβ).

Methods—Skin biopsy specimens from patients with dcSSc (n = 14) and healthy controls (n = 13) were analyzed by immunohistochemistry and immunofluorescence for TSLP, TSLP receptor, CD4, CD8, CD31, and CD163 markers. Wild-type, IL-4Rα1–, and TSLP-deficient mice were treated with TGFβ, IL-13, poly(I-C), or TSLP by osmotic pump. Human fibroblasts and peripheral blood mononuclear cells (PBMCs) were stimulated with TGFβ, IL-13, poly(I-C), or TSLP. Microarray analysis and quantitative polymerase chain reaction were performed to determine gene expression, and protein levels of phospho-Smad2 and macrophage marker CD163 were tested.

Results—TSLP was highly expressed in the skin of dcSSc patients, more strongly in perivascular areas and in immune cells, and was produced mainly by CD163+ cells. The skin of TSLP-treated mice showed up-regulated clusters of gene expression that overlapped strongly with those in IL-13– and TGFβ-treated mice. TSLP up-regulated specific genes, including CXCL9, proteasome, and interferon (IFN)–regulated genes. TSLP treatment in IL-4Rα1–deficient mice promoted similar cutaneous inflammation as in wild-type mice, though TSLP-induced arginase 1,

Address correspondence to Romy B. Christmann, MD, PhD, Boston University School of Medicine, E501 Arthritis Center, 72 East Concord Street, Boston, MA 02118-2526. romybc@bu.edu.

AUTHOR CONTRIBUTIONS

All authors were involved in drafting the article or revising it critically for important intellectual content, and all authors approved the final version to be published. Dr. Christmann had full access to all of the data in the study and takes responsibility for the integrity of the data and the accuracy of the data analysis.

Study conception and design. Christmann, Mathes, Affandi, Stifano, Lafyatis.

Acquisition of data. Christmann, Mathes, Affandi, Padilla, Nazari, Bujor, Stifano, Lafyatis.

Analysis and interpretation of data. Christmann, Mathes, Affandi, Stifano, Lafyatis.

CCL2, and matrix metalloproteinase 12 messenger RNA levels were blocked. In PBMCs, TSLP up-regulated tumor necrosis factor α, Mx-1, IFNγ, CXCL9, and mannose receptor 1 gene expression. TSLP-deficient mice treated with TGFβ showed less fibrosis and blocked expression of plasminogen activator inhibitor 1 and osteopontin 1. Poly(I-C)–treated mice showed high levels of cutaneous TSLP.

Conclusion—TSLP is highly expressed in the skin of dcSSc patients and interacts in a complex manner with 2 other profibrotic cytokines, TGFβ and IL-13, strongly suggesting that it might promote SSc fibrosis directly or indirectly by synergistically stimulating pro-fibrotic genes, or production of these cytokines.

Recruitment of T cells polarized to preferentially produce interleukin-4 (IL-4), IL-5, and IL-13, belonging to the Th2-like T subset, has been implicated in fibrosis and remodeling in systemic sclerosis (SSc) (1–3). Our recent work, analyzing peripheral blood mononuclear cells (PBMCs), identified high expression of several genes critical to IL-13 signaling by PBMCs from both patients with limited cutaneous SSc (lcSSc) and those with diffuse cutaneous SSc (dcSSc), especially in those with pulmonary arterial hypertension (PAH). Mannose receptor 1 (MRC1), an IL-13–regulated gene that is highly up-regulated on alternatively activated macrophages, was highly expressed by PBMCs from patients with SSc-associated PAH, and its expression correlated with pulmonary pressure and mortality (4). In addition, IL-13 has recently been strongly implicated in SSc skin disease (5). These data suggest that IL-13 is involved in the fibrotic pathway of SSc, but also plays a key role in the vasculopathic process, leading to PAH, a deadly complication of the disease.

Despite these observations implicating IL-13 in SSc pathogenesis, little progress has been made in identifying upstream events that ultimately lead to the Th2 profibrotic signaling in SSc. Thymic stromal lymphopoietin (TSLP) has been shown to play a crucial role in skewing T cells to a Th2 phenotype (6). TSLP is an IL-7 cytokine family member, highly produced by epithelial cells at barrier surfaces and, consequently, the first molecule produced after many disturbances in homeostasis (7). It strongly regulates immune cells such as dendritic cells, T and B cells, and granulocytes (8), and transgenic TSLP expression in the skin and lungs of mice leads to a fibrotic phenotype similar to atopic dermatitis and asthma, respectively (9,10). In addition to being tightly linked to fibrosis and possibly one of the master regulators of a Th2 phenotype, TSLP is highly induced by bacteria, viruses, and Toll-like receptor (TLR) ligands (11), and thus might play a key role in activating the immune system and in stimulating fibrosis after exposure to environmental stimuli.

We show here that TSLP is highly expressed in the skin of patients with dcSSc, mainly by immune cells in perivascular areas. In addition, we show that chronic subcutaneous stimulation of skin by TSLP activates Smad2 phosphorylation and leads to alterations in gene expression that overlap significantly with gene expression induced by transforming growth factor β (TGFβ) as well as IL-13. Examining the effects of these cytokines in IL-4Rα1– and TSLP-deficient mice revealed a striking overlap in induced gene expression and a complex interaction between these cytokines. Since poly(I-C) induced high levels of TSLP, these observations potentially link an environmental trigger, such as a TLR ligand, to SSc disease pathogenesis.

MATERIALS AND METHODS

Study participants

This study was reviewed and approved by The Boston University Medical Center Institutional Review Board. Informed consent was obtained from all subjects. A total of 14 patients with dcSSc according to diagnostic (12) and subtype (13) criteria and 13 healthy subjects were included. Skin biopsy specimens were obtained from the dorsal midforearm and fixed with formalin or used for explant fibroblast cultures.

PBMC isolation

Blood from healthy controls was collected in CPT tubes (Becton Dickinson). PBMCs were plated in 24- or 48-well plates at 37°C, at a concentration of 1–2 × 10^6 cells per well, in complete media (RPMI 1640 supplemented with 10% fetal bovine serum [FBS], 20 m*M* L-glutamine, 100 IU/ml penicillin, and 100 gm/ml streptomycin) with recombinant human IL-13 (20 ng/ml; R&D Systems), TSLP (10 ng/ml; R&D Systems), or poly(I-C) (TLR-3 ligand; 2.5 μg/ml) (InvivoGen) for from 1 hour to up to 24 hours, and lysed in RNAzol for RNA preparation.

Fibroblast culture

Primary human dermal fibroblast explant culture from healthy control subjects was established as described previously (14). Dermal fibroblasts were cultured in Dulbecco's modified Eagle's medium (DMEM) supplemented with 10% FBS and penicillin/streptomycin, and fibroblasts from passages 3 through 6 were used. Fibroblasts (100% confluent) were incubated in serum-free DMEM overnight prior to stimulation with TGFβ (2.5 ng/ml; R&D Systems), recombinant human IL-13 (20 ng/ml; R&D Systems), or TSLP (10 ng/ml; R&D Systems) for 1 hour.

RNA isolation

Total RNA from PBMCs was transferred in 600 μl of RLT buffer (Qiagen) plus β-mercaptoethanol. RNA was purified using RNeasy total kit protocol (Qiagen). Murine skin RNA was extracted using TRIzol reagent (Invitrogen). Complementary DNAs were synthesized and used for real-time quantitative polymerase chain reaction (qPCR) using primers. Quantitative PCR was performed using an ABI Prism 7700 sequence detection system (Applied Biosystems) and TaqMan assay.

Western blot analysis

Human dermal fibroblasts and mouse skin were lysed in sodium dodecyl sulfate (SDS)–polyacrylamide gel electrophoresis buffer. Equal loadings of protein samples were fractionated on SDS-polyacrylamide gels, transferred onto nitrocellulose membranes, and immunoblotted with primary antibodies, incubated with secondary antibody, and analyzed with a Luminescent Image Analyzer (LAS-4000; Fujifilm). Ponceau red and the following 3 antibodies were used: total-Smad2/3 (MW 52 and 60 kd; Cell Signaling Technology), phospho-Smad2 (MW 60 kd; Cell Signaling Technology), and β-actin (MW 42 kd; Sigma-Aldrich).

Histology, immunohistochemistry, and immunofluorescence

Briefly, for paraffinized samples, tissue sections were rehydrated, steamed with citrate buffer (BioGenex) at 99–100°C for 20 minutes, blocked and incubated with rabbit anti-human TSLP (with reactivity with mouse; LifeSpan Biosciences), rabbit anti-human TSLP receptor (LifeSpan Biosciences), or rabbit anti-mouse CD163 (Epitomics), incubated with the secondary antibody, and developed. Preincubation with TSLP peptide (Lifespan Biosciences) was used as a control. Frozen skin samples were fixed in 100% acetone, blocked, and then incubated with rabbit anti-human TSLP (LifeSpan Biosciences), Alexa Fluor 488–conjugated anti-human CD8a (BioLegend), Alexa Fluor 647–conjugated anti-human CD4, Alexa Fluor 647–conjugated anti-human CD31, and Alexa Fluor 488–conjugated anti-human CD163 antibodies. The secondary antibody was rhodamine-conjugated goat anti-rabbit antibody (Millipore). Samples were examined using a fluorescence microscope (Olympus FluoView FV10i compact self-contained confocal laser scanning microscope).

TSLP staining was rated on a scale from 0 (no TSLP staining) to 3+ (strongest staining) in 5 different regions of the skin (connective tissue and perivascular areas, epithelial cell layer, interstitial cells, and endothelial cells).

In vivo experiments

C57BL/6, BALB/c, and BALB/c-IL-4Rα1$^{-/-}$ mice were obtained from The Jackson Laboratory. C57BL/6-Taconic mice were obtained from Taconic Laboratory. C57BL/6/IFNAR$^{-/-}$ mice were obtained from Dr. John Sprent (The Scripps Research Institute, La Jolla, CA) (15). C57BL/6/IL-13$^{-/-}$ mice were kindly donated by Dr. Thomas Wynn (National Institute of Allergy and Infectious Diseases, Bethesda, MD). TSLP$^{-/-}$ mice were developed at Boston University Transgenic Core Facility with TSLP$^{-/-}$ embryos obtained from the Knockout Mouse Project Repository, and the absence of TSLP messenger RNA (mRNA) was confirmed by qPCR in the skin of all TSLP$^{-/-}$ mice (data not shown). Osmotic pumps (Alzet) designed to subcutaneously deliver phosphate buffered saline (PBS), poly(I-C) (0.1 mg), TGFβ (1.25 μg), IL-13 (4 μg), or TSLP (3 μg) were implanted in 4–8-week-old mice. After 7 or 28 days, mice were killed, and the skin (~1 cm^2) surrounding the pump outlet was homogenized in TRIzol (Invitrogen) for preparation of RNA or fixed in formalin.

Microarray analysis

All microarray data from this study have been deposited in NCBI's GEO repository (http://www.ncbi.nlm.nih.gov/geo/) (accession no. GSE34297). Micro-array data were clustered using Cluster 3.0 for Macintosh OSX, using hierarchical clustering. After selecting genes showing detectable expression in 80% of the samples, genes and the arrays were centered and normalized before clustering by gene.

Flow cytometric analysis of mouse blood and spleen

Mouse spleen was digested with 1 mg/ml collagenase D (Roche Diagnostics) in RPMI medium with depletion of red blood cells using lysing buffer (Sigma-Aldrich). Digested spleen cells were incubated with antibodies. Mouse blood was collected with 0.5*M* EDTA.

Antibodies were added directly to the blood, followed by lysis of red blood cells. Fc receptor blocker was added prior to and during staining (Innovex Biosciences). The following antibodies were used: fluorescein isothiocyanate–conjugated CD11b, phycoerythrin (PE)–conjugated CD11b, Pacific Blue–conjugated B220, PE-conjugated CD3 (all from BD Biosciences), allophycocyanin-conjugated CD115 (eBiosciences), and Alexa Fluor 647–conjugated CD11c (BioLegend). LSRII (BD Biosciences) and FlowJo software (Tree Star) were used for the analysis.

Statistical analysis

Comparisons of qPCR expression were analyzed by one-way analysis of variance and Tukey's multiple comparison post-tests. Two-group comparisons were analyzed using Student's *t*-test.

RESULTS

High expression of TSLP in the skin of patients with dcSSc

TSLP is an important upstream factor in Th2 skewing; therefore, we analyzed TSLP protein expression in the skin of dcSSc patients. TSLP was strongly expressed in dcSSc patients compared to controls (Figures 1A–D). TSLP expression in patients with dcSSc was highest in perivascular areas, where we observed inflammatory cell infiltrates, and was also seen in interstitial cells (Figures 1E and F). Expression of TSLP in the epidermis and on endothelial cells was similar between controls and dcSSc patients (data not shown). Expression of the TSLP receptor was also analyzed, and stronger expression was seen in dSSc patients than in healthy controls (results are available online at http://www.bu.edu/cort/files/2012/06/TSLP-Figures.pdf).

In order to localize the source of TSLP in the skin of dSSc patients, skin sections were double stained for TSLP and several cellular markers: CD4 and CD8 for T cells (Figures 1H and I); CD163 cells for macrophages (Figure 1K); CD31 cells for endothelium (Figure 1G), and DAPI for nuclei (Figure 1J). Immunofluorescence confirmed the expression of TSLP by immune cells around blood vessels (Figures 1G–I). TSLP colocalized most strongly with CD163+ macrophages (Figure 1K) with colocalization shown in yellow. A few CD8+ (Figure 1H) and CD4+ (Figure 1I) cells colocalized with TSLP. A blocking peptide for the anti-TSLP antibody was used as a control and clearly showed the specificity of the TSLP staining (Figures 1L–N).

TSLP shares clusters of gene expression with IL-13 and TGFβ and induces TGFβ canonical signaling in vivo

To more completely define the downstream effects of TSLP in the skin, we investigated the spectrum of the effects of TSLP in vivo. We used a murine model where TSLP was continuously released into the skin through an osmotic pump for 7 days (14) and compared TSLP with 2 other profibrotic cytokines implicated in SSc pathogenesis, IL-13 and TGFβ. Supervised clustering of genes expressed in skin treated with TSLP, IL-13, or TGFβ compared to control PBS-treated skin by microarray analysis showed that TSLP up-regulated many genes that were also up-regulated by IL-13 and TGFβ, sharing several gene

clusters (Figure 2A). In particular, some genes known to be regulated by TGFβ and up-regulated in the skin of SSc patients were up-regulated in skin from mice treated with IL-13, TGFβ, or TSLP. These included plasminogen activator inhibitor 1 (PAI-1), also known as Serpine1, thrombospondin-1, bone morphogenetic protein 1, and osteopontin 1 (SPP1) (Figure 2). In a larger series of cytokine-treated mice, we confirmed the up-regulation of one of these TGFβ-regulated genes, PAI-1, showing that PAI-1 is induced in TGFβ-treated skin (mean ± SD fold change 3.28 ± 3.25; $P = 0.03$), but is also induced in TSLP-treated and IL-13–treated skin (mean ± SD fold change 2.04 ± 0.94 and 3.28 ± 1.82; respectively; $P < 0.05$ for both) (Figure 2B).

We also confirmed coordinate up-regulation of the following genes found by microarray to be induced by all 3 cytokines: the chemokine CXCL5; secreted Frizzled-related protein 2 (sFRP-2), a Wnt family inhibitor up-regulated in human SSc skin (16); and type 2 nitric oxide synthase (NOS2), a marker of classical macrophage activation. CXCL5 was highly induced, and sFRP was moderately induced, by all 3 cytokines (Figures 2C and D). Surprisingly, NOS2 was confirmed to be up-regulated by all 3 cytokines, although modestly up-regulated by TGFβ (Figure 2E).

In addition, a specific cluster of up-regulated genes was observed only in mice treated with TSLP, including CXCL9, proteasome genes (proteasome subunit β type 10 [PSMB10] and PSMB8), guanylate binding proteins (GBP-2 and GBP-6), and several interferon (IFN)–regulated genes (IFI203, IIGP2, and IFN regulatory factor 7) (Figure 2F and Figure 3). Although not typically associated with IFN signatures, IFNγ has been shown to regulate PSMB10, PSMB8, GBP-2, and GBP-6 (17). We confirmed the selective up-regulation of CXCL9 by TSLP in a larger group of mice (mean ± SD fold change 9.30 ± 5.78 compared to control and the other 2 treatments; $P = 0.03$) (Figure 2F).

We also identified 2 small clusters of genes that were mostly up-regulated in IL-13–treated, but not TSLP-treated or TGFβ-treated, mouse skin. These clusters included arginase 1 and chitinase 3–like protein 3 (Chi3l3) genes, which were previously shown to be regulated by IL-13 (Figure 2G) (additional results are available online at http://www.bu.edu/cort/files/2012/06/TSLP-Figures.pdf). We confirmed the up-regulation of arginase 1 (mean ± SD fold change 11.07 ± 6.10; $P = 0.002$) and Chi3l3 (mean ± SD fold change 2.91 ± 0.99; $P < 0.01$) by IL-13 in a larger group of mice (Figure 2G) (additional results are available online at http://www.bu.edu/cort/files/2012/06/TSLP-Figures.pdf).

Surprisingly, we did not observe any gene cluster that was exclusively up-regulated in mice treated with TGFβ.

TSLP-induced MRC1 expression in healthy human PBMCs

We observed in our in vivo model that TSLP regulates clusters of genes that overlap with both those regulated by IL-13 and those regulated by TGFβ. We have also previously shown that MRC1, a marker for the effect of IL-13 on alternative monocyte/macrophage activation, is associated with mortality and pulmonary artery pressure in lcSSc patients and is induced by IL-13 in healthy human PBMCs (4). In order to further understand how TSLP might regulate Th2 and consequently alternatively activated macrophage skewing in SSc, we

stimulated PBMCs with IL-13, TSLP, or both and examined MRC1 mRNA expression. We observed that TSLP highly induced MRC1 expression in PBMCs (mean ± SD fold change 4.50 ± 3.12) to a similar degree as after IL-13 stimulation (fold change 6.49 ± 4.37) (P = 0.43) (Figure 4A). No significantly different additional effect was observed when both cytokines were used together (fold change 8.30 ± 4.75; P ± 0.17). In order to assess the potential effect of TSLP in the skin, we then examined dermal expression of MRC1 in dcSSc patients. We observed that MRC1 was expressed at higher levels in the skin of patients with dcSSc (fold induction 3.20 ± 1.92) than in the skin of controls (fold change 1.11 ± 0.68) ($P < 0.001$) (Figure 4B).

Kinetics of TSLP-induced gene expression by PBMCs

We showed that TSLP stimulates a unique gene signature in vivo with increased expression of proinflammatory and profibrotic genes (Figures 2 and 3). In order to better understand the kinetics of TSLP-induced gene expression, we treated PBMCs with TSLP for from 1 hour up to 24 hours and examined the expression of several genes. We confirmed that TSLP induces proinflammatory genes such as tumor necrosis factor, Mx-1, and IFNγ at early time points, followed by induction of MRC1 and CXCL9 after 8 hours (Figure 4C). Notably, IL-13 mRNA expression was not detected at any time point during the stimulation (Figure 4C).

TSLP-induced TGFβ canonical pathway activation in skin

In order to extend our in vivo data showing that TSLP increases the expression of several genes regulated by TGFβ, we examined Smad2 phosphorylation in the skin of mice treated with TSLP. Smad2 phosphorylation was induced in protein extracted from the skin of mice treated with TSLP or with TGFβ. Smad2 phosphorylation was weakly induced in mice treated with IL-13, but not in mice treated with PBS (Figure 4D).

TSLP-induced Smad2 phosphorylation in human fibroblasts

We then stimulated human dermal fibroblasts in vitro with TSLP and analyzed the effect on this TGFβ canonical pathway. We consistently observed strong up-regulation of Smad2 phosphorylation after 1 hour of TSLP stimulation, showing kinetics similar to those seen with TGFβ (Figures 4E and F).

Cutaneous inflammatory and profibrotic gene expression in TSLP-treated mice is independent of IL-13

Our in vivo microarray data showed that TSLP is probably involved in the remodeling process, up-regulating several TGFβ- and IL-13–regulated genes. Therefore, we used mice deficient in IL-4Rα1, a shared coreceptor for IL-4 and IL-13 (IL-4R$\alpha 1^{-/-}$ mice), to investigate if TSLP effects in vivo are dependent on IL-13 signaling. Hematoxylin and eosin (H&E) analysis showed a similar inflammatory reaction in the skin in TSLP-treated mice in the absence of IL-4Rα1 compared to the TSLP-treated wild-type mice, with a large infiltration of immune cells mainly in the subcutaneous tissue in both groups compared to mice treated with PBS. In addition, TSLP-treated IL-4Rα1–deficient mice and wild-type mice showed a similar increase in CD163+ infiltrating macrophages (Figures 5A–F).

IL-4Rα1 deletion blocked expression of a subset of TSLP-induced genes. TSLP up-regulated IL-13, IL-1β, and NOS2 expression in the skin of IL-4Rα1–deficient and wild-type mice to a similar degree (fold change for IL-13, 8.20 in wild-type mice versus 11.94 in IL-4Rα1$^{-/-}$ mice [Figure 5G]; for IL-1α, 2.85 in wild-type mice versus 1.72 in IL-4Rα1$^{-/-}$ mice [Figure 5K]; for NOS2, 17.49 in wild-type mice versus 11.58 in IL-4Rα1$^{-/-}$ mice [Figure 5L]). Deletion of IL-4Rα1 also had no significant effect on TSLP-induced expression of profibrotic genes, such as PAI-1 (mean ± SD fold change 4.49 ± 1.41 in wild-type mice versus 2.66 ± 1.22 in IL-4Rα1$^{-/-}$ mice; $P = 0.16$) (Figure 5M) and SPP1 (mean ± SD fold change 2.08 ± 0.64 in wild-type mice versus 1.80 ± 0.16 in IL-4Rα1$^{-/-}$ mice; $P = 0.54$) (Figure 5N). In contrast, expression of the following genes was blocked or partially blocked in TSLP-treated IL-4Rα1–deficient mice compared to wild-type mice: CCL2 (mean ± SD fold change 26.16 ± 3.66 in wild-type mice versus 14.36 ± 6.99 in IL-4Rα1$^{-/-}$ mice; $P = 0.04$), arginase 1 (6.17 ± 1.09 in wild-type mice versus 0.71 ± 0.14 in IL-4Rα1$^{-/-}$ mice; $P = 0.001$), and matrix met-alloproteinase 12 (158.00 ± 8.10 in wild-type mice versus 0.88 ± 0.72 in IL-4Rα1$^{-/-}$ mice; $P < 0.01$) (Figures 5H–J).

Since IL-13 has also been reported to promote fibrosis through IL-13Rα2, we tested the effect of TSLP-treatment in IL-13–deficient mice. TSLP stimulated expression of PAI-1, NOS2, and arginase 1 in IL-13–deficient mice to a similar level as in wild-type mice (results are available online at http://www.bu.edu/cort/files/2012/06/TSLP-Figures.pdf), suggesting that the inhibition of arginase 1 seen in IL-4Rα1 mice was mediated by IL-4 rather than IL-13. In contrast, CCL2 mRNA expression induced by TSLP in wild-type mice was not induced in IL-13$^{-/-}$ mice (results are available online at http://www.bu.edu/cort/files/2012/06/TSLP-Figures.pdf).

We also investigated whether the profibrotic effects of TSLP were dependent on either type I or type II IFN by treating mice deficient in the type I IFN receptor or IFNγ (IFNAR$^{-/-}$ and IFN$\gamma^{-/-}$) with TSLP. Up-regulation of PAI-1 and CXCL5 by TSLP was not affected by the absence of either of these receptors (results are available online at http://www.bu.edu/cort/files/2012/06/TSLP-Figures.pdf).

TGFβ effects in vivo are partially dependent on TSLP

We showed above that TSLP in vivo up-regulates several TGFβ- and IL-13–regulated genes and activates the canonical TGFβ pathway in vitro. Therefore, we used TSLP-deficient mice to investigate if the profibrotic effects of TGFβ were dependent on TSLP signaling (see Materials and Methods). TSLP-deficient mice had no observable phenotype and no apparent immune developmental deficiency, confirmed by flow cytometric analysis of B cell, T cell, and macrophage markers in the blood and spleen (results are available online at http://www.bu.edu/cort/files/2012/06/TSLP-Figures.pdf).

Surprisingly, the profibrotic effect of TGFβ manifest by the presence of a small nodule at the outlet of the pump observed in all TGFβ-treated wild-type mice was not seen in TSLP$^{-/-}$ mice. This macroscopic observation was confirmed by H&E staining (Figures 6A–C), showing thinner dermis in the TSLP$^{-/-}$ mice treated with TGFβ (mean ± SD 396.66 ± 134.87 μm) compared to the wild-type mice (504.54 ± 78.91 μm; $P = 0.03$) (Figure 6D). Several profibrotic genes were totally blocked in TGFβ-treated TSLP-deficient mice. These

included PAI-1 (10.08 ± 4.76 in wild-type mice versus 0.62 ± 0.25 in TSLP$^{-/-}$ mice; P = 0.01) (Figure 6E), osteopontin/SPP1 (20.30 ± 8.06 in wild-type mice versus 0.78 ± 0.29 in TSLP$^{-/-}$ mice; P = 0.04) (Figure 6F), and Wnt-1–inducible signaling pathway protein 1 (data not shown). Of note, wild-type mice treated with TGFβ showed an induction of TSLP mRNA expression in the skin compared to that of mice treated with PBS (data not shown).

High levels of TSLP in the skin in an innate immune SSc murine model

Consistent with the notion that SSc is triggered by an environmental stimulus, possibly infectious, we have previously shown that chronic subcutaneous poly(I-C) causes skin fibrosis with features similar to SSc (14). Therefore, we analyzed the expression of TSLP in the skin in this model by immunohistochemistry. TSLP was highly expressed in infiltrating immune cells in the skin of poly(I-C)–stimulated mice (Figure 6H) compared to PBS-treated mice (Figure 6G), thus showing a similar pattern to that observed in the skin of patients with dcSSc. Preincubation with a blocking peptide for the anti-TSLP antibody was used as a control (Figure 6I).

Complex interaction among IL-13, TGFβ, and TSLP

Based on our findings and on the data from the literature, poly(I-C), a TLR-3 ligand, strongly induces TSLP (10). TSLP then induces inflammation independently of IL-13, induces IL-4/IL-13–regulated genes through IL-13 signaling, and ultimately leads to up-regulation of several profibrotic genes, similar to TGFβ. More importantly, the profibrotic effects of TGFβ are partially dependent on TSLP signaling and induce TSLP-positive feedback (Figure 6J).

DISCUSSION

This study supports the notion that TSLP is a key factor in the Th2 proinflammatory and profibrotic profiles in SSc, since it was highly expressed by perivascular inflammatory cells in SSc skin. In addition, our findings show that TSLP up-regulates profibrotic gene expression in vivo, similarly to TGFβ, and activates canonical TGFβ signaling and plays a key role in TGFβ signaling in vivo, suggesting that TSLP regulates TGFβ or that the TSLP receptor is able to cross-activate Smad2 phosphor-ylation. Our findings show that TSLP has a dual effect in vivo and in vitro, stimulating both proinflammatory and profibrotic processes.

Epithelial cells, which highly express TSLP in allergic Th2-based disorders, such as atopic dermatitis and asthma (18), were originally identified as the principal source of TSLP. More recently, several studies have shown that TSLP can be expressed by other cell types, including fibroblasts, mast cells, CD68+ macrophages (19,20), and dendritic cells (21). In our study, we observed strong expression of TSLP in the skin of dcSSc patients mainly in immune cells, colocalizing with CD163+ cells, a marker for resident activated macrophages (22), and also colocalizing with a few CD4+ and CD8+ T cells. Mononuclear cell infiltration has been shown to be key in several fibrotic diseases, including SSc (4,23). Therefore, high cutaneous expression of TSLP by immune cells in SSc patients might be pivotal in perpetuating the immune system activation through TSLP-activated dendritic cells (8),

further attracting mononuclear cells, and inducing T cell production of Th2-derived interleukins and chemokines, creating a profibrotic Th2 environment (20). Thus, immune cell expression of TSLP may be more important than epithelial cell expression in fibrotic diseases such as SSc.

TSLP expression by immune cells might be triggered by an environmental stimulus, possibly infectious, and TSLP expression can be highly induced by TLR ligands, mainly poly(I-C), a TLR-3 ligand (11). Notably, we found that TSLP was primarily induced in infiltrating inflammatory cells in the skin of our murine SSc-like poly(I-C) model, associated with skin inflammation and fibrosis. Together, these observations suggest that TSLP could be induced by innate immune stimuli and subsequently, activate both inflammatory and profibrotic processes involved in SSc pathogenesis.

In addition, our in vivo and in vitro results suggest that TSLP stimulates similar gene expression and intracellular pathways as TGFβ. In particular, we found several clusters of genes that were up-regulated by both of these cytokines in vivo. Furthermore, we found that TSLP strongly up-regulates Smad2 phosphorylation, both in vivo and in vitro. Since Smad2 phosphorylation occurs directly downstream from the type I TGFβ receptor and is part of the canonical signaling pathway, these results strongly suggest that TSLP up-regulates TGFβ activity. Notably, TGFβ profibrotic gene expression in vivo was strongly blocked in the absence of TSLP signaling, confirming a complex interaction between TSLP and TGFβ. Thus, a detailed understanding of the interaction between the key cytokines IL-13, TGFβ, and TSLP is urgent and essential for targeting these cytokines for the treatment of fibrotic diseases such as SSc.

The potential importance of TSLP in fibrotic skin disease was further reinforced by other observations. TSLP stimulated PBMCs to express MRC1, an important monocyte/macrophage alternative activation marker, as effectively as stimulation with IL-13. Supporting our results, we also observed increased cutaneous levels of mRNA for MRC1, suggesting that TSLP might stimulate MRC1 expression in SSc skin. However, we cannot exclude the possibility that MRC1 expression in SSc skin is regulated by another mediator, such as IL-13, which we have shown is increased in the circulation of SSc patients and also stimulates MRC1. In addition, in mice deficient in IL-13/IL-4 signaling, TSLP failed to induce some Th2-regulated genes, showing that some effects of TSLP are mediated by IL-4/IL-13. However, many genes induced by TSLP, including profibrotic and proinflammatory genes, were unaltered in both IL-4Rα1– and IL-13–deficient mice, indicating that these cytokines are not required for many TSLP effects.

A recent study of an IL-13–transgenic model of atopic dermatitis also relates directly to our findings. Increased inflammatory cells and skin remodeling with collagen deposition characterize this model. It was shown that TSLP, but not IL-13, was relevant for the induction of fibrosis (24). In IL-4Rα1–deficient mice, the profibrotic cutaneous effects of TSLP were not dependent on IL-13 signaling. In addition, in the absence of IL-13 signaling, TSLP still induced as strong cutaneous inflammation and skin damage as observed in TSLP-treated wild-type mice. Arginase 1, an alternatively activated macrophage marker, was induced in the skin of BALB/c mice treated with TSLP, although not in C57BL/6 mice,

which was likely a strain effect since BALB/c mice are more prone to skewing of the ratio of Th2 cells to alternatively activated macrophages than are C57BL/6 mice (25). Consistent with findings previously reported in the literature, arginase 1 expression was dependent on the presence of IL-4Rα1 (26). Thus, TSLP might play a key role in inducing profibrotic mediators and in amplifying IL-13 signaling, and may also be critical to inflammatory pathways that do not depend on IL-13.

In addition to its overlapping effects with IL-13 and TGFβ on gene expression, TSLP induced a distinct set of genes in murine skin, including CXCL9, a gene whose expression we had previously shown is increased in SSc skin (14). We showed that TSLP also induces CXCL9 by PBMCs in vitro, consistent with the results of a previous study where high levels of proteasomes, chemokines including CXCL9, and IL-13–regulated genes were observed in PBMCs stimulated with TSLP (27). We showed that TSLP rapidly stimulates proinflammatory gene expression by PBMCs followed by induction of a more profibrotic marker, MRC1.

In conclusion, TSLP might represent one of the first responses to innate immune activation in dermal fibrosis, and might play a key role in SSc after exposure to an unknown trigger. TSLP might contribute to activating the immune system toward both proinflammatory and profibrotic processes as observed in SSc patients, strongly interacting with IL-13 and TGFβ signaling, perpetuating the response. Of particular note, this study highlights the importance of TSLP in TGFβ-mediated fibrosis.

Acknowledgments

We thank Yuriy Alekseyev, PhD (Department of Pathology and Laboratory Medicine) and Marc Lenburg, PhD (Section of Computational Biomedicine) of the Boston University Microarray Resource Core Facility for performing all microarray-based experiments and help with data analysis. We also thank Dr. Thomas A. Wynn (Chief, Immunopathogenesis Section) of the National Institute of Allergy and Infectious Diseases for the donation of IL-13–deficient mice.

Supported by the NIH (National Institute of Arthritis and Musculoskeletal and Skin Diseases grant 1P50-AR-060780-02 to Bos-ton University Medical Center and grant 2R01-AR-051089-06A1 to Dr. Lafyatis). Dr. Christmann's work was supported by an Arthritis Foundation Postdoctoral Fellowship Award. Mr. Affandi's work was supported by the Dutch Arthritis Association (Reumafonds grant NR-10-1-301) and the Netherlands Organization for Scientific Research (NWO Mosaic grant 017.008.014).

References

1. Ripke S, Sanders AR, Kendler KS, Levinson DF, Sklar P, Holmans PA, et al. the Schizophrenia Psychiatric Genome-Wide Association Study (GWAS) Consortium. . Genome-wide association study identifies five new schizophrenia loci. Nat Genet. 2011; 43:969–76. [PubMed: 21926974]
2. Hasegawa M, Fujimoto M, Kikuchi K, Takehara K. Elevated serum levels of interleukin 4 (IL-4), IL-10, and IL-13 in patients with systemic sclerosis. J Rheumatol. 1997; 24:328–32. [PubMed: 9034992]
3. Granel B, Chevillard C, Allanore Y, Arnaud V, Cabantous S, Marquet S, et al. Evaluation of interleukin 13 polymorphisms in systemic sclerosis. Immunogenetics. 2006; 58:693–9. [PubMed: 16832637]
4. Christmann RB, Hayes E, Pendergrass S, Padilla C, Farina G, Affandi AJ, et al. Interferon and alternative activation of monocyte/macrophages in systemic sclerosis–associated pulmonary arterial hypertension. Arthritis Rheum. 2011; 63:1718–28. [PubMed: 21425123]

5. Li Q, Wang W, Yamada T, Matsumoto K, Sakai K, Bando Y, et al. Pleural mesothelioma instigates tumor-associated fibroblasts to promote progression via a malignant cytokine network. Am J Pathol. 2011; 179:1483–93. [PubMed: 21763682]
6. Comeau MR, Ziegler SF. The influence of TSLP on the allergic response. Mucosal Immunol. 2010; 3:138–47. [PubMed: 20016474]
7. Ziegler SF, Artis D. Sensing the outside world: TSLP regulates barrier immunity. Nat Immunol. 2010; 11:289–93. [PubMed: 20300138]
8. Watanabe N, Hanabuchi S, Soumelis V, Yuan W, Ho S, de Waal Malefyt R, et al. Human thymic stromal lymphopoietin promotes dendritic cell-mediated $CD4^+$ T cell homeostatic expansion. Nat Immunol. 2004; 5:426–34. [PubMed: 14991051]
9. Yoo J, Omori M, Gyarmati D, Zhou B, Aye T, Brewer A, et al. Spontaneous atopic dermatitis in mice expressing an inducible thymic stromal lymphopoietin transgene specifically in the skin. J Exp Med. 2005; 202:541–9. [PubMed: 16103410]
10. Zhou B, Comeau MR, De Smedt T, Liggitt HD, Dahl ME, Lewis DB, et al. Thymic stromal lymphopoietin as a key initiator of allergic airway inflammation in mice. Nat Immunol. 2005; 6:1047–53. [PubMed: 16142237]
11. Kato A, Favoreto S Jr, Avila PC, Schleimer RP. TLR3- and Th2 cytokine-dependent production of thymic stromal lymphopoietin in human airway epithelial cells. J Immunol. 2007; 179:1080–7. [PubMed: 17617600]
12. Subcommittee for Scleroderma Criteria of the American Rheumatism Association Diagnostic and Therapeutic Criteria Committee. . Preliminary criteria for the classification of systemic sclerosis (scleroderma). Arthritis Rheum. 1980; 23:581–90. [PubMed: 7378088]
13. Furst DE, Clements PJ, Steen VD, Medsger TA Jr, Masi AT, D'Angelo WA, et al. The modified Rodnan skin score is an accurate reflection of skin biopsy thickness in systemic sclerosis. J Rheumatol. 1998; 25:84–8. [PubMed: 9458208]
14. Farina GA, York MR, Di Marzio M, Collins CA, Meller S, Homey B, et al. Poly(I:C) drives type I IFN- and TGFβ-mediated inflammation and dermal fibrosis simulating altered gene expression in systemic sclerosis. J Invest Dermatol. 2010; 130:2583–93. [PubMed: 20613770]
15. Kolumam GA, Thomas S, Thompson LJ, Sprent J, Murali-Krishna K. Type I interferons act directly on CD8 T cells to allow clonal expansion and memory formation in response to viral infection. J Exp Med. 2005; 202:637–50. [PubMed: 16129706]
16. Bayle J, Fitch J, Jacobsen K, Kumar R, Lafyatis R, Lemaire R. Increased expression of Wnt2 and SFRP4 in Tsk mouse skin: role of Wnt signaling in altered dermal fibrillin deposition and systemic sclerosis. J Invest Dermatol. 2008; 128:871–81. [PubMed: 17943183]
17. Foss GS, Prydz H. Interferon regulatory factor 1 mediates the interferon-γs induction of the human immunoproteasome subunit multicatalytic endopeptidase complex-like 1. J Biol Chem. 1999; 274:35196–202. [PubMed: 10575004]
18. Zeuthen LH, Fink LN, Frokiaer H. Epithelial cells prime the immune response to an array of gut-derived commensals towards a tolerogenic phenotype through distinct actions of thymic stromal lymphopoietin and transforming growth factor-β. Immunology. 2008; 123:197–208. [PubMed: 17655740]
19. Hirano R, Hasegawa S, Hashimoto K, Haneda Y, Ohsaki A, Ichiyama T. Human thymic stromal lymphopoietin enhances expression of CD80 in human $CD14^+$ monocytes/macrophages. Inflamm Res. 2011; 60:605–10. [PubMed: 21274737]
20. Soumelis V, Reche PA, Kanzler H, Yuan W, Edward G, Homey B, et al. Human epithelial cells trigger dendritic cell mediated allergic inflammation by producing TSLP. Nat Immunol. 2002; 3:673–80. [PubMed: 12055625]
21. Kashyap M, Rochman Y, Spolski R, Samsel L, Leonard WJ. Thymic stromal lymphopoietin is produced by dendritic cells. J Immunol. 2011; 187:1207–11. [PubMed: 21690322]
22. Lau SK, Chu PG, Weiss LM. CD163: a specific marker of macrophages in paraffin-embedded tissue samples. Am J Clin Pathol. 2004; 122:794–801. [PubMed: 15491976]
23. Wick G, Backovic A, Rabensteiner E, Plank N, Schwentner C, Sgonc R. The immunology of fibrosis: innate and adaptive responses. Trends Immunol. 2010; 31:110–9. [PubMed: 20106721]

24. Oh MH, Oh SY, Yu J, Myers AC, Leonard WJ, Liu YJ, et al. IL-13 induces skin fibrosis in atopic dermatitis by thymic stromal lymphopoietin. J Immunol. 2011; 186:7232–42. [PubMed: 21576506]

25. Kuroda E, Kito T, Yamashita U. Reduced expression of STAT4 and IFN-γ in macrophages from BALB/c mice. J Immunol. 2002; 168:5477–82. [PubMed: 12023341]

26. Loke P, Nair MG, Parkinson J, Guiliano D, Blaxter M, Allen JE. IL-4 dependent alternatively-activated macrophages have a distinctive in vivo gene expression phenotype. BMC Immunol. 2002; 3:7. [PubMed: 12098359]

27. Urashima M, Sakuma M, Teramoto S, Fuyama Y, Eto Y, Kondo K, et al. Gene expression profiles of peripheral and cord blood mononuclear cells altered by thymic stromal lymphopoietin. Pediatr Res. 2005; 57:563–9. [PubMed: 15746263]

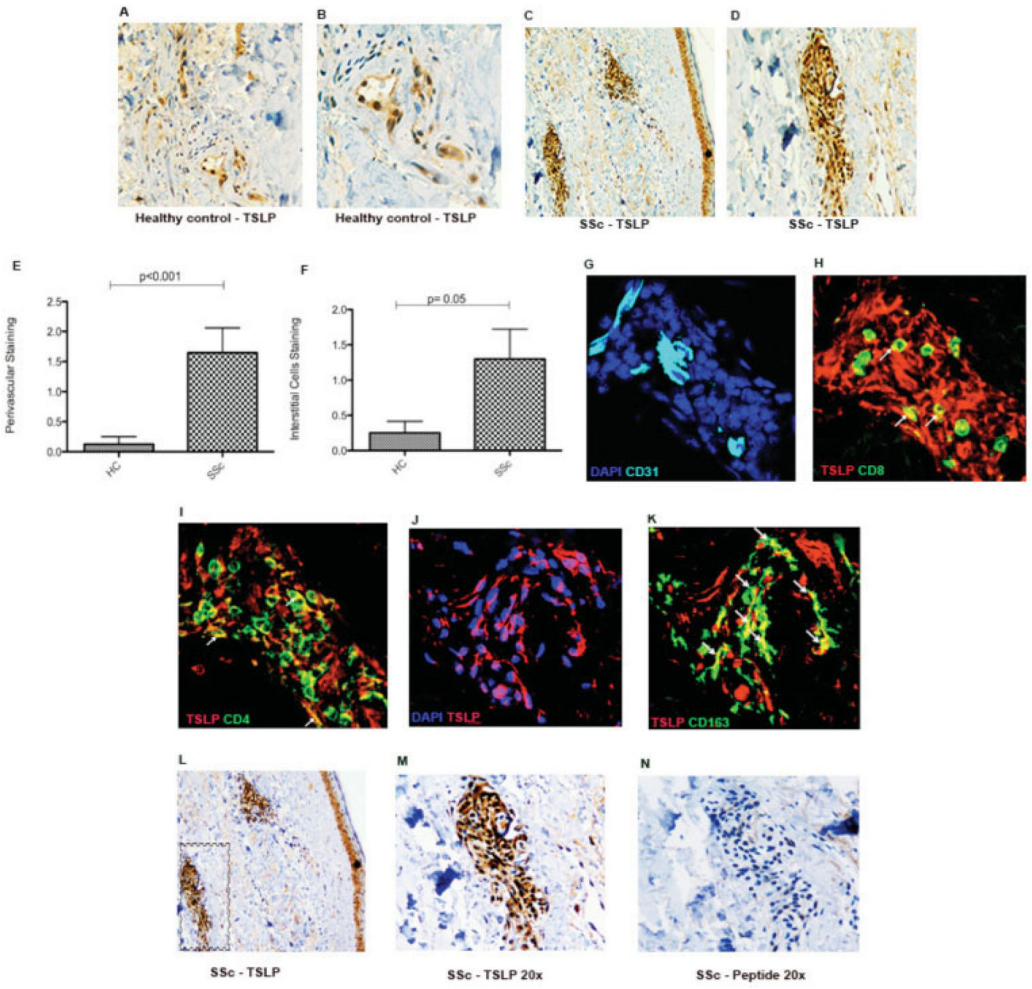

Figure 1.

Representative images of thymic stromal lymphopoietin (TSLP) expression in the skin of patients with diffuse cutaneous systemic sclerosis (dcSSc). **A**, Skin from a healthy control (HC) showing TSLP staining in brown with a vessel on the bottom right. Original magnification × 10. **B**, Higher-magnification view of the vessel in **A**, showing positive TSLP staining on endothelial cells. Original magnification × 20. **C**, Skin from a dcSSc patient showing TSLP staining in brown with positive staining on interstitial cells and on the vessels on the bottom left and upper right. Original magnification × 10. **D**, Higher-magnification view of the left vessel in **C**, showing positive staining on endothelial cells and in the perivascular area. Original magnification × 20. **E** and **F**, Scores for TSLP-positive staining of the perivascular area (**E**) and interstitial cells (**F**) in skin samples from healthy controls (n = 10) and SSc patients (n = 11). Bars show the mean ± SEM. **G–K**, Representative images of immunofluorescence analysis of skin samples from dcSSc patients stained for DAPI in blue and CD31 in cyan (**G**), stained for CD8+ cells in green, TSLP in red, and a few cells colocalizing with TSLP in yellow (**arrows**) (**H**), stained for CD4+ cells in green, TSLP in red, and a few cells colocalizing with TSLP in yellow (**arrows**) (**I**), stained for DAPI in blue, TSLP in red, and cells colocalizing with TSLP in purple (**J**), and

stained for CD163+ cells in green, TSLP in red, and cells colocalizing with TSLP in yellow (**arrows**) (**K**). Original magnification × 60. **L**, TSLP-positive staining (brown) in 2 perivascular areas and in the epithelial cell layer. Original magnification × 10. **M**, TSLP-positive staining (brown) in the perivascular area shown in the boxed area in **L**. Original magnification × 20. Sections shown in **L** and **M** were incubated with rabbit anti-human polyclonal antibody. **N**, Staining of the area shown in **H** with peptide-blocked anti-TSLP control (TSLP synthetic peptide; negative staining).

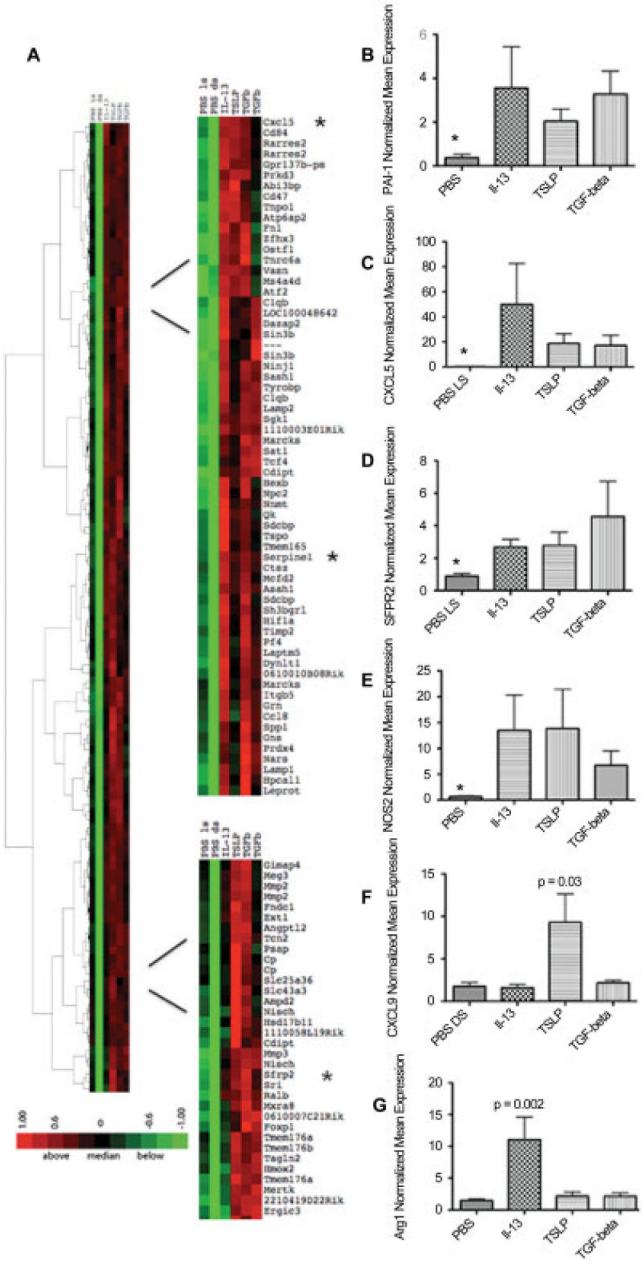

Figure 2.

Gene expression in mouse skin after treatment with interleukin-13 (IL-13), thymic stromal lymphopoietin (TSLP), and transforming growth factor β (TGFβ) via 7-day subcutaneous pump. **A**, Two main clusters showing several genes highly expressed in all 3 treatment groups (IL-13, TSLP, and TGFβ) compared to control (phosphate buffered saline [PBS]–treated local skin [LS] and PBS-treated distal skin [DS]). Several genes were analyzed by quantitative polymerase chain reaction to confirm their high expression in the skin of mice receiving each treatment (n = 3 in the PBS, IL-13, and TGFβ groups; n = 6 in the TSLP group; 2 independent experiments). Green represents low expression; red represents high expression. **B–G**, Expression of mRNA for plasminogen activator inhibitor 1 (PAI-1) (**B**),

CXCL5 (**C**), secreted Frizzled-related protein 2 (sFRP-2) (**D**), type 2 nitric oxide synthase (NOS2) (**E**), CXCL9 (**F**), and arginase 1 (Arg1) (**G**). * = $P = 0.03$ versus all other groups in **B**, **D**, and **E**; * = $P < 0.01$ versus all other groups in **C**. *P* values are versus PBS in **F** and **G**. Values are the mean ± SEM fold change normalized to mRNA expression in 1 PBS-treated sample.

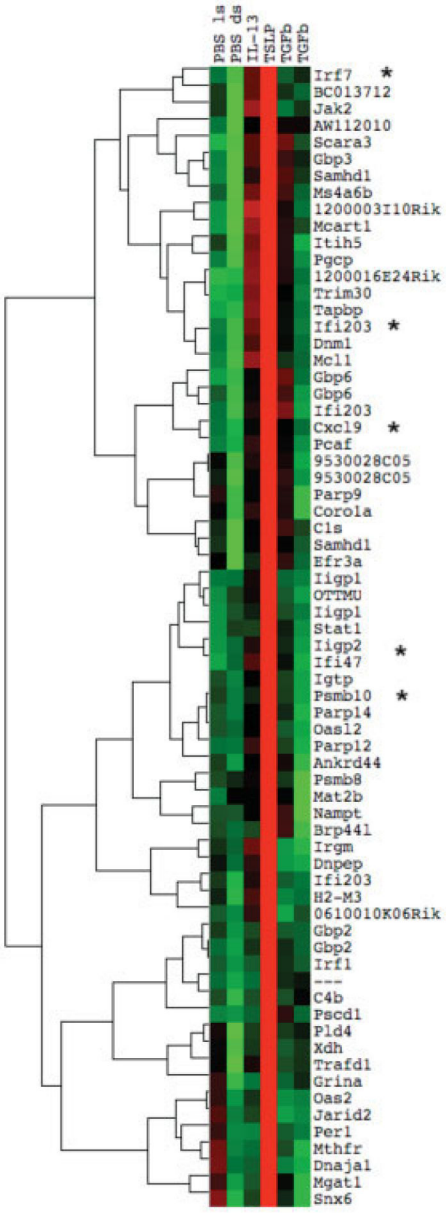

Figure 3.

Gene expression in mouse skin samples after treatment with interleukin-13 (IL-13), thymic stromal lymphopoietin (TSLP), or transforming growth factor β (TGFβ) via 7-day subcutaneous pump. A unique TSLP cluster was seen, with several interferon-regulated genes (indicated by **asterisks**) highly expressed exclusively in TSLP-treated mouse skin. Green represents low expression; red represents high expression. PBS = phosphate buffered saline; ls = local skin; ds = distal skin.

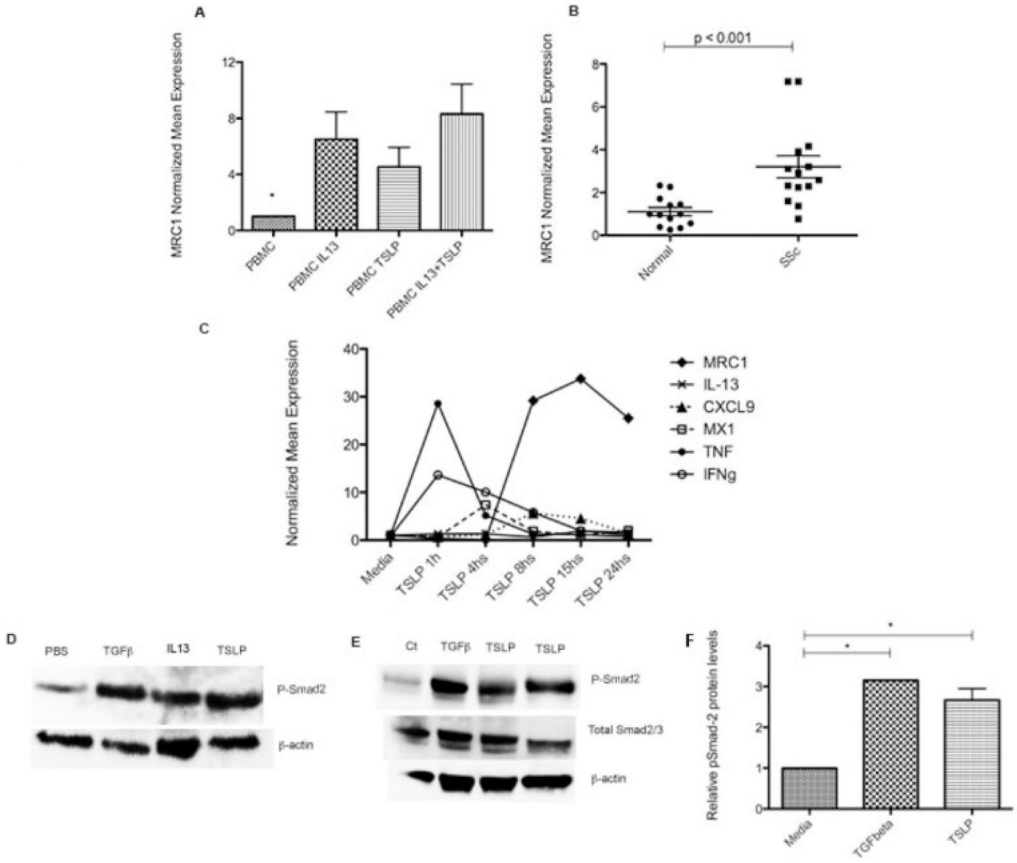

Figure 4.

A, Mannose receptor 1 (MRC1) expression in peripheral blood mononuclear cells (PBMCs) from 5 healthy controls, stimulated for 18 hours with interleukin-13 (IL-13; 20 ng/ml), thymic stromal lymphopoietin (TSLP; 10 ng/ml), or both. Media alone was used as a control. Bars show the mean ± SEM fold change normalized to mRNA expression in controls. * = $P < 0.001$ versus all other groups. **B**, MRC1 expression in skin samples from 14 patients with diffuse cutaneous systemic sclerosis (SSc) and 13 healthy controls. Each data point represents a single subject; horizontal lines show the mean and SEM. **C**, Gene expression in PBMCs from 3 healthy controls, stimulated for 1–24 hours with TSLP (10 ng/ml) using media alone as a control. Values are the mean ± SEM fold change normalized to mRNA expression in the control. TNF β tumor necrosis factor; IFN γ = interferon-γ. **D**, Higher expression of pSmad2 in the skin of mice subjected to transforming growth factor β (TGFβ), IL-13, and TSLP pump than in mice subjected to phosphate buffered saline (PBS) pump. **E**, Increased expression of pSmad2 in healthy human dermal fibroblasts stimulated for 1 hour with TGFβ (2.5 ng/ml) or TSLP (10 ng/ml) after overnight starvation at 100% confluence and compared to media alone (Ct). Results are representative of 5 independent experiments. In **D** and **E**, blotted proteins were probed with rabbit anti-pSmad2 monoclonal antibody, total Smad2/3 antibody, and secondary antibody, and visualized using enhanced chemiluminescence. As a control for equal protein loading, the membrane was stripped and reprobed for β-actin using a monoclonal antibody for β-actin. **F**, Expression of pSmad2,

quantified by scanning densitometry and corrected for levels of β-actin in the same samples of human dermal fibroblasts. Bars show the mean ± SEM. * = $P < 0.05$.

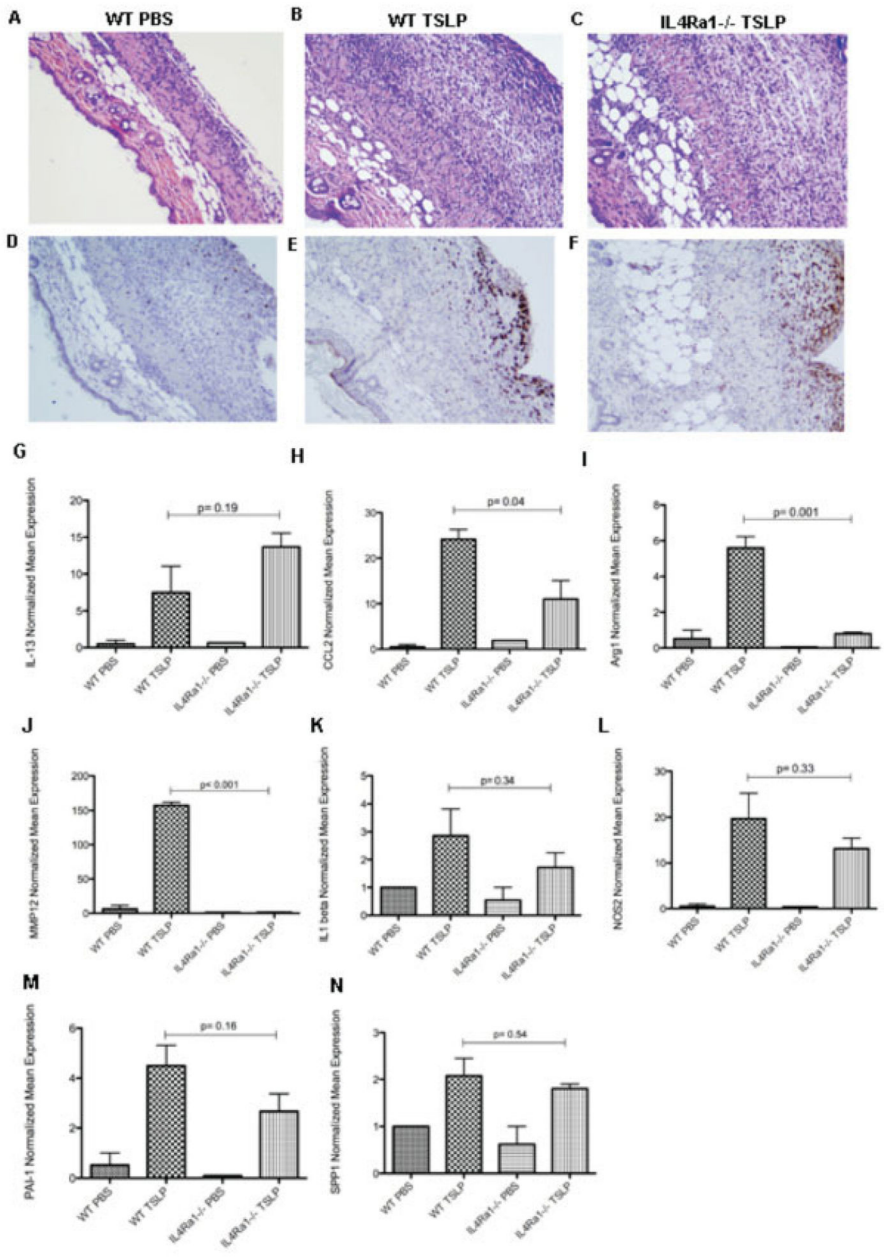

Figure 5.

Skin involvement after 7 days of thymic stromal lymphopoietin (TSLP) treatment in wild-type (WT) and IL-4Rα1–deficient mice. **A–C**, Representative images of hematoxylin and eosin–stained skin sections from a phosphate buffered saline (PBS)–treated wild-type mouse, showing preservation of all skin layers (**A**), a TSLP-treated wild-type mouse, showing cell infiltration (**B**), and a TSLP-treated IL-4R$\alpha 1^{-/-}$ mouse, showing intense cell infiltration (**C**). Original magnification × 10. **D–F**, Representative images of CD163-stained skin sections from a PBS-treated wild-type mouse (**D**), a TSLP-treated wild-type mouse, showing strong CD163 staining in brown on cells in the subcutaneous layer (**E**), and a TSLP-treated IL-4R$\alpha 1^{-/-}$ mouse, showing CD163-positive staining similar to that in **E** (**F**).

Original magnification × 10. **G–N**, Expression of mRNA for interleukin-13 (IL-13) (**G**), CCL2 (**H**), arginase 1 (Arg1) (**I**), matrix metalloproteinase 12 (MMP-12) (**J**), IL-1α (**K**), type 2 nitric oxide synthase (NOS2) (**L**), plasminogen activator inhibitor 1 (PAI-1) (**M**), and osteopontin (SPP1) (**N**). Bars show the mean ± SEM fold change normalized to mRNA expression in 1 PBS-treated wild-type mouse sample (n = 3 samples per group).

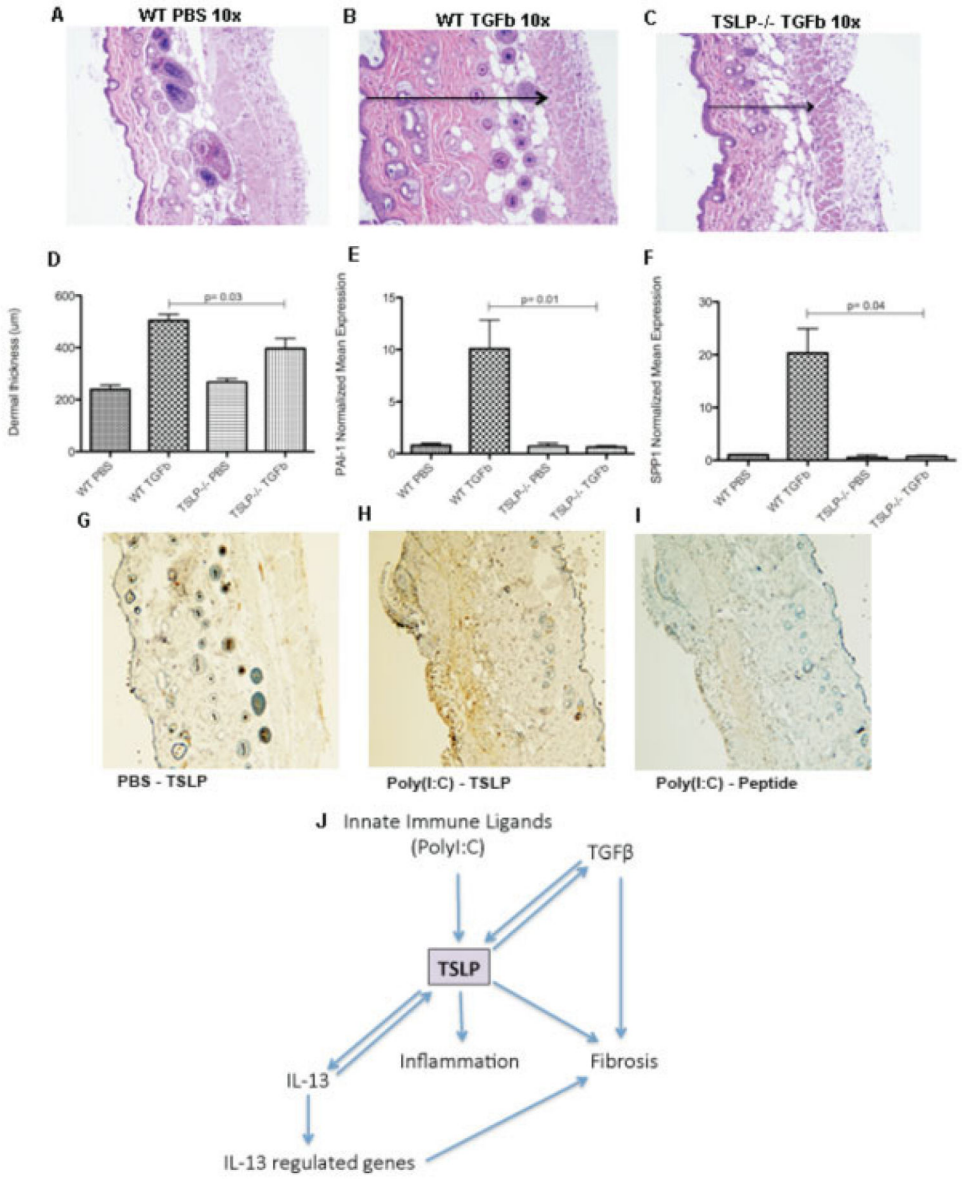

Figure 6.

The in vivo profibrotic effects of transforming growth factor β (TGFβ) are partially dependent on thymic stromal lymphopoietin (TSLP). **A–C**, Representative images of hematoxylin and eosin–stained skin sections from a phosphate buffered saline (PBS)–treated wild-type (WT) mouse, showing preservation of the structures (**A**), a TGFβ-treated wild-type mouse, showing the dermal thickness (**arrow**), measured as the distance between the muscle and the epidermal layers (**B**), and a TGFβ-treated TSLP$^{-/-}$ mouse, showing a reduction in the dermal thickness (**arrow**) (**C**). Original magnification × 10. **D**, Dermal thickness, measured as the distance between the muscle and the epidermal layers. **E** and **F**, Expression of mRNA for plasminogen activator inhibitor 1 (PAI-1) (**E**) and osteopontin (SPP1) (**F**). **G–I**, Representative images of TSLP-stained skin sections from a PBS-treated control mouse showing low TSLP expression and preserved presence of the annexes (**G**), a

mouse treated with poly(I-C) for 28 days (systemic sclerosis immune model), showing strong expression of TSLP staining in brown and thickening of the dermis with loss of the annexes (**H**), and a poly(I-C)–treated mouse with peptide-blocked anti-TSLP control negative staining (**I**). Original magnification × 10. **J**, Schematic representation of the complex interaction of TSLP with interleukin-13 (IL-13) and TGF*β*.